Available online at www.sciencedirect.com

ScienceDirect

Procedia Structural Integrity 1 (2016) 034–041

Structural Integrity Procedia

www.elsevier.com/locate/procedia

1st International Conference on Structural Integrity

Rotary Fatigue Testing to Determine the Fatigue Life of NiTi alloy Wires: An Experimental and Numerical Analisys

André Carvalho[a], Manuel Freitas[a,*], Luis Reis[a], Diogo Montalvão[b], Manuel Fonte[a,c]

[a]*IDMEC - Instituto Superior Técnico, Universidade de Lisboa, Av. Rovisco Pais, 1, 1049-001 Lisboa, Portugal*
[b]*School of Engineering and Technology, University of Hertfordshire, College Lane Campus, Hatfield, Herts AL10 9AB, UK*
[c]*Escola Náutica Infante D. Henrique, Av. Eng. Bonneville Franco, 2770-058, Paço d'Arcos, Portugal*

Abstract

Endodontic rotary file instruments used to treat root canals in dentistry suffered breakthrough transformations in recent years when stainless steel was replaced by Nickel-Titanium (NiTi). NiTi alloys used in Endodontics possess superelastic properties at body temperature (37C) that bring many advantages on the overall performance of the root-canal treatment. They can follow curved root canals more easily than stainless steel instruments and have been reported to be more effective in the removal of the inflamed pulp tissue and protection of the tooth structure. However, these instruments eventually fracture under cyclic bending loading due to fatigue, without any visible signals of degradation to the practitioner. This problem brought new challenges on how new instruments should be tested, as NiTi alloys are highly non-linear and present a large hysteresis cycle in the Elastic domain. Current existing standards are only available for Stainless Steel testing. Thus, many authors have attempted to design systems that can test NiTi endodontic files under fatigue loads. However, no approach has been universally adopted by the community yet, as in most cases they are based on empirical set ups. Following a more systematic approach, this work presents the results of rotary fatigue tests for several NiTi wires from different manufacturers (Memry™ and Euroflex™).The formulation is presented, where the material strength reduction can be quantified from the determination of the strain and the number of cycles until failure, as well numerical FEM simulation to verify the analytical model predictions.

Peer-review under responsibility of the Scientific Committee of PCF 2016.

Keywords: Fatigue; Files; NiTi wires; Life evaluation.

1. Introduction

In dentistry, the root canal procedure is done using a rotary file that removes the existing nerve endings on a tooth. In the past, endodontic files used in this procedure were made from highly flexible steel alloys. However, steel alloy files, while being flexible, are still too rigid to avoid damaging the walls of the root canals. In order to minimize these adverse effects, Nickel-Titanium alloys are now being used in the design of endodontic rotary files instead of stainless steel alloys. NiTi alloys are superelastic metal alloys that are able to fully recover from large deformations (up to

* Corresponding author.
E-mail address: mfreitas@dem.ist.utl.pt

Peer review under responsibility of the Scientific Committee of PCF 2016.
10.1016/j.prostr.2016.02.006

strains of 10% Montalvão et al. (2014)). These alloys, however, have a drawback when compared to steel files: their fatigue life is relatively shorter than steel and, as seen in commercial endondontic files, they break without a previous mechanical warning, increasing the risk of the file failing inside the teeth.

There are some studies to determine the fatigue life of NiTi alloys, through traditional uniaxial fatigue tests and rotary bending fatigue tests Plotino et al. (2009). Rotary bending tests are the tests that most accurately replicate the kind of loads and deformation a file is subjected to when inside a root canal. The great majority of the existing machines in the literature only perform the fatigue test with a predetermined set of shapes. However, most of the imposed deformations are far from the complex shapes of the root canals. Plotino et al. (2009).

Of special interest is the rotary fatigue machine designed by Cheung and Darvell Cheung and Darvell (2007). This machine consists of three pins that can be positioned manually to deform the endondontic file. The file is then put into rotation using a contra-angle. This type of machine has an advantage of being more versatile than the more common machines with simulated canal carved in a stainless steel plate, where one can have only one predetermined curvature per plate De-Deus et al. (2010); Gambarini et al. (2012); Lopes et al. (2010); Plotino et al. (2010)

In this work, an automated configurable rotary bending-testing machine was designed. This testing machine was designed to adapt and change the degree of bending from simple point bending to more complex multi-point bending. The machine consists in three pairs of pins positioned by servomotors, which deform the specimen into a desired complex shape. The specimen is then put into rotation until failure is detected.

The machine design also enables rotary bending tests with constant curvature (constant strain) along a segment. With a constant strain, one can compare directly the result with the more common uniaxial fatigue tests. Also, one can perform tests in different regions of the superelastic stress-strain curve, enabling an estimation of the stress and the metallic phase of the alloy during the test.

2. Designing the Testing Machine

The testing machine was designed to be versatile and to offer a wide range of possible bending configurations. Based in the machine designed by Cheung and Darvell Cheung and Darvell (2007), the testing machine has three pins that can be configured to make 1 to 4 point bending tests. In our machine, however, the pins are positioned at configurable locations using servo-motors. Configurable positioning enables a greater precision and repeatability, while providing a simple interface (Fig. 1).

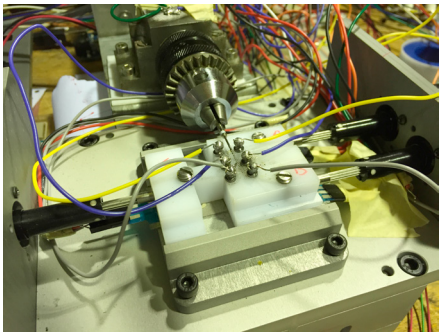

Fig. 1: Testing area with an endondontic file.

For the rotation of the specimens, a brushless DC motor with variable speed is used instead of the more common contra-angle. With a standalone DC motor, one can control the velocity of the test more precisely and automatically. The motor is able to do tests from 100rpm (16.67Hz) to 3000rpm (50Hz), which covers the range of most NiTi endodontic files with a drive speed usually between 150 and 350rpm.

To detect when the specimen fail (whether it is wire or an endondontic file), an electronic failure detection system was implemented. This system uses the natural conductivity of NiTi alloys to detect any failure by constantly monitoring the level of voltage between the specimen and each pin. When the circuit is open it means that the specimen failed and the test stops automatically.

3. Positioning control and Constant Curvature

The most important aspect of this machine is its ability to generate bending configurations automatically. The configurations are set by positioning the pins (Fig. 1) in order to deform the specimen into a shape (Fig.2). The

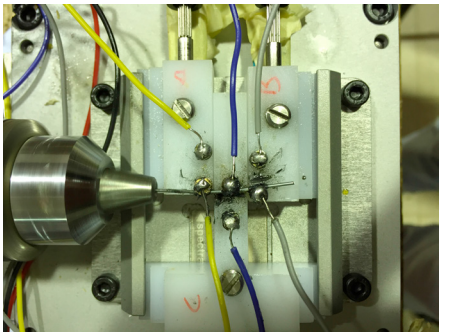

Fig. 2: Wire deformed during a test.

machine software enables two positioning modes: individual pin positioning and constant curvature radius generation.

3.1. Constant Curvature Generation for Wire Specimens

The main advantage of having a constant curvature in a uniform beam is that in that region the strain is also constant and proportional to the radius as in (1).

$$\epsilon_x = -z\frac{1}{\rho} \tag{1}$$

where ρ is the radius of curvature, ϵ_x is the strain along the length of the beam and z is the distance to the neutral surface.

Using the Euler-Bernoulli beam theory to obtain the analytical model of the wire, we obtain the deflection for the wire. For an infinitesimal element (1) becomes:

$$\epsilon_x(x) = -z\frac{\mathrm{d}^2 w}{\mathrm{d}x^2} \tag{2}$$

However, we want a constant strain level for an entire segment of the specimen and, consequently, the position of the pins must be determined in to generate a constant strain section.

Using a standard square minimization algorithm to find the pin displacements needed for the desired constant strain level in the specimens mid section, while minimizing the overall deformation, we obtain the three pin positions Carvalho et al. (2015). We also have to take into account the influence of thickness of the wire and the requirement that the wire must be tangent to the pins at all times. This leads to a variable distance between the contact point at the surface and the neutral surface Carvalho et al. (2015). Adding this requirement to the optimization algorithm, we obtain deformation profiles similar to the one in Fig. 3.

For the case of Fig. 2, which corresponds to setting the desired strain to 2%, the curvature can be seen in Fig. 4. Knowing that the internal radius of the pins is $1\mathrm{mm}$ and using (1), we obtain that the angle of the arc is $\approx 11.71\,\mathrm{deg}$ and the radius of curvature is $50\mathrm{mm}$. These two parameters can be used to compare results with testing methods such as the Pruet et al Pruett et al. (1997).

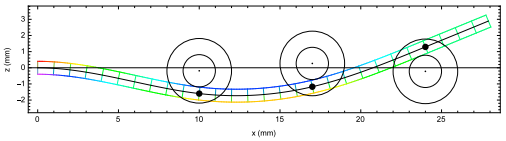

Fig. 3: Beam under a desired constant strain of 2%, with color-coded strain and tangent pins.

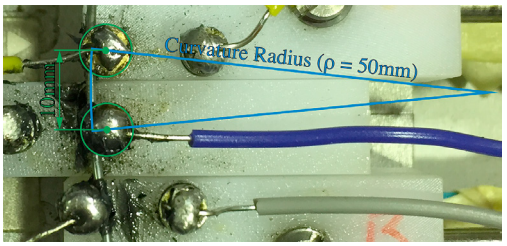

Fig. 4: Deformed wired with a desired strain of 2% superimposed with the curvature radius.

4. Results for a NiTi Wire

The first materials to be tested in the rotary fatigue machine were a Memry™ and a Euroflex™ wires, both with a diameter of 0.8mm. The wires, when under an uniaxial load, has the stress-strain relation in Fig. 5.

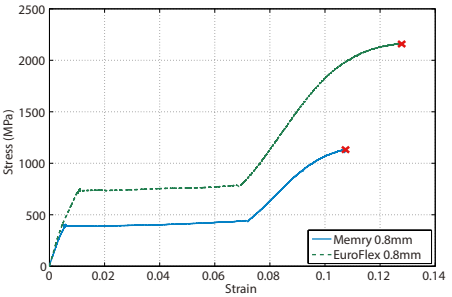

Fig. 5: Uniaxial tension test of the Memry™ 0.8mm diameter wire.

Figure 5 has three distinct regions: a first austenitic elastic region, a horizontal elastic region with a mixture of austenitic and martensitic phases (also known as R-phase) and a final plastic martensitic region. Another characteristic of these Ni-Ti alloys is that they exhibit a large hysteresis when unloading occurs. For simplicity sake, this phenomenon was not considered in the study of the fatigue of the wire specimens.

The fatigue tests were concentrated on the first two regions, imposing strains level from 0.8% to 6%. The results can be seen in Fig. 6. The specimens with strains smaller or equal to 1% (corresponding to the first zone in the stress-strain plot in Fig. 5) show a large fatigue life when compared with the rest of the points, with two specimens never failing. The remaining points show a decrease of the fatigue life as the imposed strain increases. The specimen with the largest strain showed a life of 34 cycles for the Memry™ wire and 16 cycle for the Euroflex™ wires.

5. NUMERICAL SIMULATIONS

Numerical simulations using FEA (Finite Element Analysis) can contribute to a better understanding of the failure mechanisms of the Ni-Ti wires in the proposed testing machine. Also, they allow predicting the stress distribution on the wire more accurately than the Euler-Bernoulli beam theory approximation, since SMA (Shape Memory Alloy) or superelastic material properties are highly non-linear.

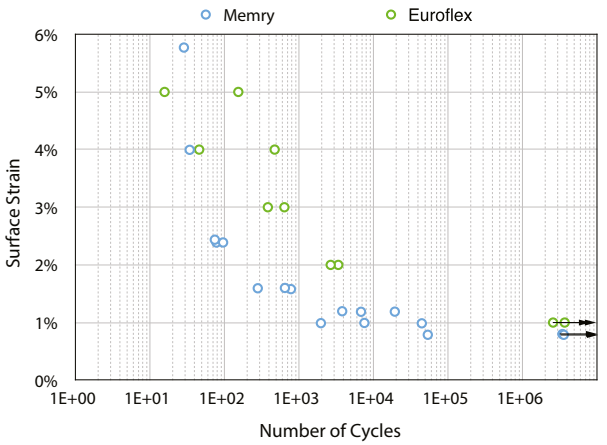

Fig. 6: Strain vs. number of cycles for a Memry™ 0.8mm diameter wire.

5.1. Model

A static structural FEA was conducted in ANSYS 16.1 Workbench with the model shown in Fig. 7 to replicate the experiments conducted in the testing machine. The 0.8mm diameter wire was modelled with 1632 solid elements with superelastic material properties Carvalho et al. (2015); Yin et al. (2015) introduced in the projects Engineering Data cell as shown in Table 1. The wire was clamped at one end and it was deformed under bending using three steel actuator pins that moved in the y direction based on the constant curvature formulation earlier presented. The movement of the actuators was simulated as being gradual, in an explicit iterative way. Contact properties were added between the actuator pins and the wire, with a considered frictional coefficient of 0.2.

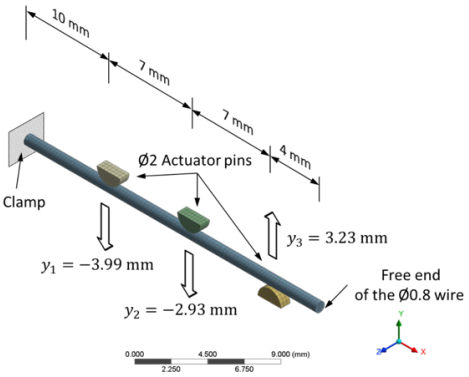

Fig. 7: Mesh, boundary conditions and loads (displacements) for the FEA model.

5.2. Results

The assessment of the results will be based on the normal stress in the x direction, since the beam is in pure bending on the xy plane with the loads being applied in the y direction. The maximum stress in the x direction for both materials during loading and unloading is plotted in Fig. 8.

Fig. 8 shows that the behaviour of the alloys is non-linear and follows what is expected for a superelastic alloy. However, the maximum values for the normal stress is being determined to be near the clamping region according to the FEA results. This should not be a surprise, because the clamping is modelled as being infinitely rigid. This may also lead to a stress concentration location, reason why the values can be quite significant. Since the true clamping region

Table 1: Material properties for the Memry™ and Euroflex™ alloys introduced in ANSYS Workbench projects Engineering Data project cell.

Material Property	Memry™	Euroflex™
Isotropic Elasticity		
Young Modulus (GPa)	70	70
Poisson's Ratio	0.33	0.33
Superelasticity		
Sigma SAS (MPa)	368	736
Sigma FAS (MPa)	484	798
Sigma SSA (MPa)	232	337
Sigma FSA (MPa)	100	135
Epsilon (mm/mm)	0.063	0.059
Alpha	0	0

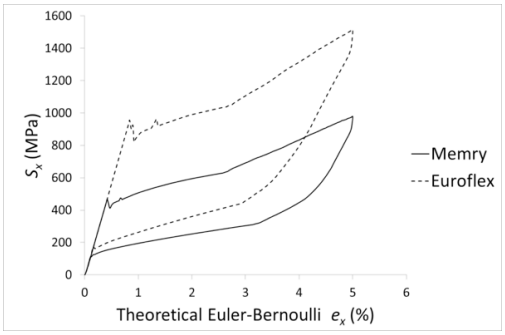

Fig. 8: Maximum normal stress in the x direction S_x.

is very difficult to be modelled accurately and the wires failed near the 1st and the 2nd pins during the experiments (in an apparently random fashion), the following analysis neglects the clamping location.

Fig. 9 shows a few examples of the normal stress distribution in the x direction on the Memry™ (Figs. 9a to 9c) and Euroflex™ (Fig. 9d to 9f) wires respectively for different loading conditions. It is observed that the normal stress (hence the normal strain) in the x direction is approximately constant in the constant curvature region between actuator pins 1 and 2, validating the theoretical formulation assumptions.

Notwithstanding, what is noteworthy to mention is that the maximum compression stress (identified as Min in Fig. 9) was consistently determined to be near the first actuator pin and larger than the maximum traction stress (identified as Max in Fig. 9). This might be due to a frictional contact property that was added between the pins and the wire as an attempt to mimic the existing testing machine.

The maximum traction stress seems to be randomly floating within the constant strain curvature region, i.e., it can either be near the first pin, near the second pin, or in between the two pins. Being a constant strain region, the floating of the maximum traction stress location can only be attributed to numerical error. Therefore, it is expected that the wires will fracture near either pin 1 or pin 2 due to friction, being more likely to fail near pin 1.

6. Fracture Surfaces

The fracture surfaces of the specimens tested in the rotary testing bending machine were observed on a Scanning Electronic Microscopy, JEOL existent at MicroLab from IST. For comparison purposes, the fracture surface of the specimens tested in uniaxial tension was also observed. Fig. 10 show respectively, the general view of the fracture

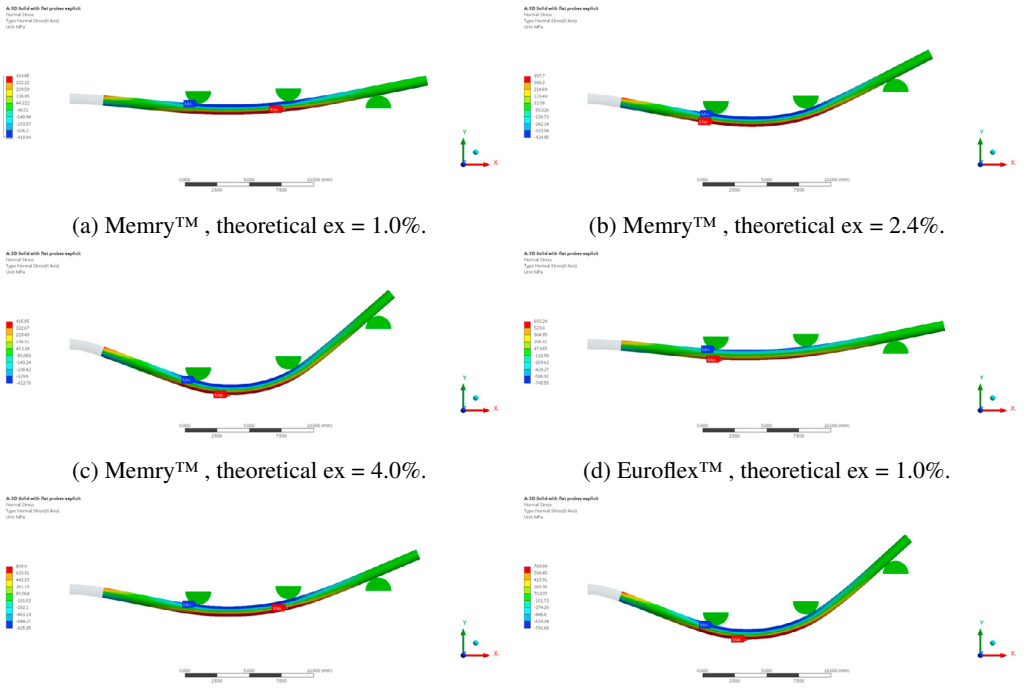

(a) Memry™ , theoretical ex = 1.0%. (b) Memry™ , theoretical ex = 2.4%.

(c) Memry™ , theoretical ex = 4.0%. (d) Euroflex™ , theoretical ex = 1.0%.

(e) Euroflex™ , theoretical ex = 2.0%. (f) Euroflex™ , theoretical ex = 4.0%.

Fig. 9: Maximum normal stress in the x direction S_x

surface of the uniaxial tension specimen Memry™ 0.8 mm and the amplification of the fracture surface where a characteristic ductile facies can be observed with dimples developed during the failure process.

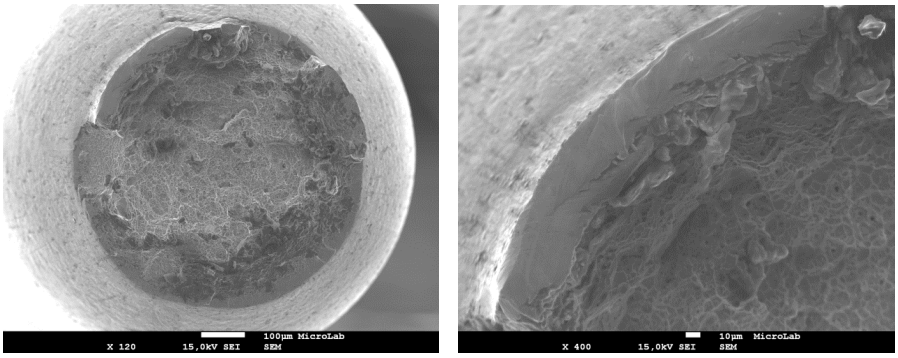

(a) General view (b) Amplification of the fracture surface

Fig. 10: Uniaxial tension

The fracture surfaces observed in fatigued specimens are substantially different from the uniaxial testing ones and are characterized by flat fractures surfaces, as usually observed in failed specimens under rotating bending conditions. For lower cycles to failure a very small fatigue zone is observed near the surface. As the number of cycles to failure increases, the fatigue zone on the specimens also increases. Fig. 11a shows the fractured surface of the specimen of Memry™ 0.8 mm failed by fatigue at 44551 cycles. A clear focus of crack initiation can be observed and is shown in detail on Fig. 11b which is significantly different from Fig. 10b. Therefore these NiTi alloy fractured at rotating bending fatigue do not differ from fractured surfaces by fatigue in more classic isotropic metals.

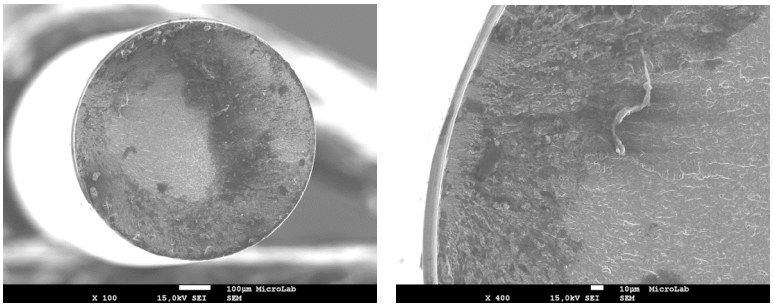

(a) Failure at 44551 cycles (b) Crack initiation

Fig. 11: Rotary bending fatigue

7. CONCLUSIONS

The work presented on this paper presents a testing apparatus designed to perform rotary fatigue tests on NiTi endondontic files and wires. The testing machine was designed to be versatile, enabling a series of testing configurations and test types, using computer controlled automatic positioning of system that bends the specimens into user supplied shapes or into a bending configuration that has a constant strain section. A series of fatigue tests were done using a Memry™ and Euroflex™ $0.8\mathrm{mm}$ diameter wires. The wires showed a very long fatigue life (most of the specimens did not fail) when under strain levels in the elastic austenitic phase. When imposing strain in the R-phase region, the fatigue life of the wire drastically reduced, with fatigue life ranging from 20,000 (lower strain levels) to 16 cycles (higher strain levels).

For future work, other wires with different diameters will be tested, as well different endondontic files.

Acknowledgements

This work was supported by national funds through FCT - Fundação para a Ciência e a Tecnologia as part of the project PTDC/EME/AME/122795/2010.

References

Carvalho, A., Freitas, M., Reis, L., Montalvão, D., Fonte, M., 2015. Rotary fatigue testing machine to determine the fatigue life of NiTi alloy wires and endondontic files. Procedia Engineering 114, 500 – 505.

Cheung, G. S. P., Darvell, B. W., 2007. Fatigue testing of a niti rotary instrument. part 1: strain-life relationship. International endondontic Journal 40, 612–618.

De-Deus, G., Moreira, E. J. L., Lopes, H. P., elias, C. N., 2010. Extended cyclic fatigue life of F2 ProTaper instruments used in reciprocating movement. International endondontic Journal 43, 1063–1068.

Gambarini, G., Gergi, R., Naaman, A., Osta, N., Al Sudani, D., 2012. Cyclic fatigue analisys of twisted file rotary niti instruments used in reciprocating motion. International endondontic Journal 45, 802–806.

Lopes, H. P., Britto, I. M. O., elias, C. N., de Oliveira, J. C. M., Neves, M. A. S., Moreira, E. J. L., Siqueira, J. F., 2010. Cyclic fatigue resistance of protaper universal instruments when subjected to static and dynamic tests. Oral Surg Oral Med Oral Pathol Oral Radiol Endod 110, 401–404.

Montalvão, D., Alçada, F., Fernandes, F., Correia, S., 2014. Structural characterisation and mechanical fe analysis of conventional and m-wire ni–ti alloys used in endondontic rotary instruments. The Scientific World Journal: Materials Science.

Plotino, G., Grange, N. M., Cordaro, M., Testarelli, L., Gambarini, G., 2009. A review of cyclic fatigue testing of nickel-titanium rotary instruments. Cyclic Fatigue or Rotary Instruments 35 (1), 1469–1476.

Plotino, G., Grange, N. M., Melo, M. C., Bahia, M. G., Testarelli, L., Gambarini, G., 2010. Cyclic fatigue of niti rotary instruments in a simulated apical abrupt curvature. International endondontic Journal 43, 226–230.

Pruett, J., Clement, D., Carnes, D., 1997. Cyclic fatigue testing of nickel titanium endodontic instruments. Journal of Endodontics 23, 77–85.

Yin, W., Sczerzenie, F., Long, M., Belden, C., Manjeri, R., Lafond, R., 2015. Structure and properties of large diameter hot rolled NiTi bars for seismis applications. SAES Smart Materials, New Harthford, New York.